Kidney International, Vol. 53 (1998), pp. 136–145

De novo glomerular osteopontin expression in rat crescentic glomerulonephritis

HUI Y. LAN, XUE Q. YU, NIANSHENG YANG, DAVID J. NIKOLIC-PATERSON, WEI MU, RAIMUND PICHLER, RICHARD J. JOHNSON, and ROBERT C. ATKINS

Department of Nephrology, Monash Medical Centre, Clayton, Victoria, Australia; Department of Nephrology, The First Hospital, Sun Yat-Sen University of Medical Sciences, Guangzhou, China; and Division of Nephrology, University of Washington School of Medicine, Seattle, Washington, USA

***De novo* glomerular osteopontin expression in rat crescentic glomerulonephritis.** Osteopontin (OPN) is a secreted acidic glycoprotein that has potent monocyte chemoattractant and adhesive properties. Up-regulation of tubular OPN expression is thought to promote interstitial macrophage infiltration in experimental nephritis; however, the role of OPN in glomerular lesions, particularly crescent formation, is unknown. The present study used Northern blotting, *in situ* hybridization and immunohistochemistry to examine OPN expression in a rat model of accelerated anti-GBM glomerulonephritis. Osteopontin mRNA and protein is expressed by some parietal epithelial cells, thick ascending limbs of Henle and medullary tubules and collecting ducts in normal rat kidney. *De novo* OPN mRNA and protein expression was evident in glomerular visceral and parietal epithelial cells in anti-GBM glomerulonephritis. Glomerular OPN expression preceded and correlated with macrophage infiltration in the development of hypercellularity, focal and segmental lesions and, notably, crescent formation. There was marked up-regulation of OPN expression by tubular epithelial cells that also preceded and correlated with interstitial macrophage ($r = 0.93$, $P < 0.001$) and T-cell infiltration ($r = 0.85$, $P < 0.001$). Both glomerular and tubular OPN expression correlated significantly with proteinuria ($P < 0.001$) and a reduction in creatinine clearance ($P < 0.01$). In addition, double immunohistochemistry showed co-expression of osteopontin and one of its ligands, CD44, in intrinsic renal cells. CD44 and OPN expression by parietal epithelial cells was evident in crescent formation, while virtually all OPN-positive tubules expressed CD44. Infiltrating macrophages and T-cells were CD44-positive, but only a small proportion of T-cells and few macrophages showed OPN expression. Interestingly, strong OPN mRNA and protein expression was seen in macrophage multinucleated giant cells. In summary, this study suggests that OPN promotes macrophage and T-cell infiltration in the development of renal lesions in rat anti-GBM glomerulonephritis, including glomerular crescent and multinucleated giant cell formation.

Osteopontin (OPN) is a highly acidic, phosphorylated, secreted glycoprotein which contains an adhesive arginine-glycine-aspartic acid (RGD) sequence [1, 2]. Osteopontin is expressed in a constitutive or inducible fashion by a number of cell types, including: osteoclasts, various epithelia, macrophages, T lymphocytes, smooth muscle cells and some tumors [3–8]. A number of different forms of OPN have been described in various cell types that result from alternative RNA splicing and post-translational modifications such as glycosylation, phosphorylation and proteolytic cleavage [1, 2]. Osteopontin is a cell adhesion and migration molecule and functions through binding to a number of ligands including the $\alpha_v\beta_3$ integrin (vitronectin receptor), extracellular matrix proteins such as collagen type I and fibronectin, and CD44 [1, 2, 9]. The adhesive properties of OPN have been implicated in a diverse array of biological responses such as bone absorption, inhibition of renal stone formation, tumor metastasis and macrophage recruitment at sites of inflammation [8, 10–13]. Furthermore, OPN and its proteolytic fragments have been shown to have potent chemotactic activity [14, 15]. Indeed, the subcutaneous injection of OPN into mice induces prominent monocyte infiltration [13].

Macrophage infiltration plays an important role in the pathogenesis of many types of kidney disease [16]. Much interest has, therefore, been focused on the mechanisms by which macrophages are recruited into the kidney and interact with intrinsic kidney cell types. Examination of experimental models of glomerular and interstitial nephritis have found that the development of interstitial macrophage infiltration is almost exclusively restricted to areas of tubular damage in which there is marked up-regulation of tubular OPN mRNA and protein expression [17–22]. However, the potential importance of OPN in the pathogenesis of macrophage-mediated glomerular lesions, such as crescent formation, and the relationship between OPN and CD44 expression in glomerulonephritis have not been addressed. Therefore, we studied a rat model of crescentic glomerulonephritis in order to determine (*1*) whether OPN contributes to the development of glomerular lesions, and (*2*) the relationship between expression of OPN and one of its ligands, CD44, in disease development.

METHODS

Experimental disease model

Accelerated anti-GBM glomerulonephritis was induced in inbred male Sprague-Dawley rats (150 to 200 g) as previously described [23]. Briefly, animals were immunized s.c. with 5 mg normal rabbit IgG in Freund's complete adjuvant and injected i.v. with 10 ml/kg rabbit anti-rat GBM serum (12.5 mg IgG/ml) five days later (termed day 0). Groups of 6 rats were killed at three

Key words: osteopontin, crescentic glomerulonephritis, anti-GBM glomerulonephritis, lesions.

Received for publication June 26, 1997
and in revised form August 25, 1997
Accepted for publication August 27, 1997

hours, and days 1, 7, 14 or 21 after administration of nephrotoxic serum. In addition, a group of 6 normal rats was studied.

Histopathology

Tissues for histology were fixed in 4% formalin and 4 μm paraffin sections were stained with hematoxylin and eosin (H&E) or periodic acid-Schiff reagent (PAS). The percentage of glomeruli exhibiting atrophy/segmental sclerosis, global sclerosis or glomerular crescentic formation was assessed by examination of at least 100 glomerular cross sections (gcs) per animal in PAS-stained sections. Glomerular hypercellularity was assessed on the basis of total glomerular cell counts per glomerular cross-section. At least 100 glomeruli per animal were scored on H&E stained sections and ranked as follows: (0) normal (less than 50 cells/gcs); (1) mild (60 to 80 cells/gcs); (2) moderate (80 to 120 cells/gcs); (3) severe hypercellularity (more than 120 cells/gcs). Cortical tubular atrophy and fibrosis were semiquantitatively analyzed on PAS stained sections and graded on a scale of 0 to 3 as follows: (0) no apparent damage; (1) mild damage, with lesions involving less than 15% of the cortex; (2) moderate damage, involving 15% to 30% of the cortex; (3) severe damage, that is, involving more than 30% of the cortex and focal accumulation of leukocytes at sites of damage.

Renal function and proteinuria

Urinary protein excretion in 24 hour collections was determined using the Manual Ponceau Red method. Concentrations of plasma and urine creatinine were measured using the standard Jaffe rate reaction (alkaline picrate). All analyses were performed by the Department of Biochemistry, Monash Medical Centre.

Antibodies

Mouse monoclonal antibodies (mAb) used were: MPIIIB10, anti-rat OPN (obtained from the Developmental Studies Hybridoma Bank, Iowa City, IA, USA); ED1, anti-rat CD68, labels monocytes and macrophages [24, 25]; R73, anti-rat αβ T-cell receptor non-polymorphic determinant [26]; OX-50, anti-rat CD44 which recognizes all forms of CD44 [27, 28]. Peroxidase- and alkaline phosphatase-conjugated goat anti-mouse IgG, mouse peroxidase anti-peroxidase complexes (PAP), and mouse alkaline phosphatase anti-alkaline phosphatase complexes (APAAP) were purchased from Dakopatts (Glostrup, Denmark).

Immunohistochemistry

Double immunostaining was performed on 4 μm paraffin sections of formalin-fixed kidney using a microwave-based method of multiple immunoenzymatic staining, which has been described in detail elsewhere [29]. Briefly, sections were dewaxed, placed in 0.01 M sodium citrate buffer pH 6.0 and heated for 2 × 5 minutes in a microwave oven at 2450 MHz and a power output of 800 watts. This facilitates retrieval of cytoplasmic antigens. Sections then were labeled with the ED1 mAb using a 3 layer PAP method and developed with 3,3-diaminobenzidine to give a brown product. Sections then were microwave heated a second time to denature bound IgG molecules on the section, inactivate endogenous alkaline phosphatase and prevent antibody cross-reaction [29]. Sections were labeled with the MPIIIB10 mAb using a 3 layer APAAP method and developed with Fast Blue BB Base (Sigma Chemical Co., St. Louis, MO, USA), giving a blue product.

Double immunostaining was also performed on cryostat sections of tissue fixed in 2% paraformaldehyde-lysine-periodate. In this case, sections were labeled with OX-50 or R73 mAb with a 3 layer PAP method before the sections were microwave treated, and then stained with ED1 or MPIIIB10 mAb and developed with a 3 layer APAAP method.

All sections were counterstained with periodic acid-Schiff (PAS) reagent without hematoxylin and coverslipped in an aqueous mounting medium. An isotype-matched mouse antibody 73.5 against human CD45R was used as the negative control.

Probes

A 1 kb cRNA probe was generated from the 2B7 cDNA clone of rat smooth muscle osteopontin [7]. Sense and anti-sense cRNA probes were labeled with digoxigenin (DIG)-UTP using a T7 RNA polymerase kit (Boehringer Mannheim GmbH, Mannheim, Germany). In addition, a 358 bp fragment of rat glyceraldehyde-3-phosphate dehydrogenase (GAPDH) cDNA was amplified by reverse transcription PCR and labeled with DIG-dUTP using the High-Prime random priming kit (Boehringer Mannheim GmbH). Probes were precipitated and incorporation of DIG was determined by dot blotting.

Northern blot analysis

Northern blotting was performed as previously described [30]. Briefly, total cellular RNA was extracted using the RNAzol reagent (Gibco BRL, Gaithersburg, MD, USA), and 20 μg samples were denatured with glyoxal and dimethylsulphoxide, size fractionated on 1.2% agarose gels and capillary blotted onto positively-charged nylon membranes (Boehringer Mannheim). Membranes were hybridized overnight at 68°C or 42°C with DIG-labeled cRNA or cDNA probes, respectively, in a DIG Easy Hyb solution (Boehringer Mannheim). Following hybridization, membranes were washed finally in 0.1 × SSC/0.1% SDS at 68°C or 0.2 × SSC/0.1% SDS at 42°C. Bound probes were detected using sheep anti-DIG antibody (Fab) conjugated with alkaline phosphatase and development with CPD-star enhanced chemiluminescence (Boehringer Mannheim). Chemiluminescence emissions were captured on Kodak XAR film and densitometry analysis performed using the public domain NIH ImagePC program (developed at the U.S. National Institutes of Health and available on the Internet at http://rsb.info.nih.gov/nih-image/).

In situ hybridization

In situ hybridization was performed on 4 μm paraffin sections of formalin-fixed tissue using a microwave-based protocol as described in detail elsewhere [31, 32]. After dewaxing, sections were treated with a microwave oven for 2 × five minutes as described above, incubated with 0.2 M HCl for 15 minutes, followed by 1% Triton X-100 for 15 minutes, and then digested for 20 minutes with 10 μg/ml Proteinase-K at 37°C (Boehringer Mannheim). Sections then were washed in 2 × SSC, prehybridized, and then hybridized with 0.3 ng/μl DIG-labeled sense or anti-sense OPN cRNA probe overnight at 37°C in a hybridization buffer containing 50% deionized formamide, 4 × SSC, 2 × Denhardt's solution, 1 mg/ml salmon sperm DNA, and 1 mg/ml yeast tRNA. Sections were washed finally in 0.1 × SSC at 37°C and the hybridized probe detected using sheep anti-DIG antibody (Fab) conjugated with alkaline phosphatase and color development with NBT/X-phosphate (Boehringer Mannheim). Sections were mounted in an

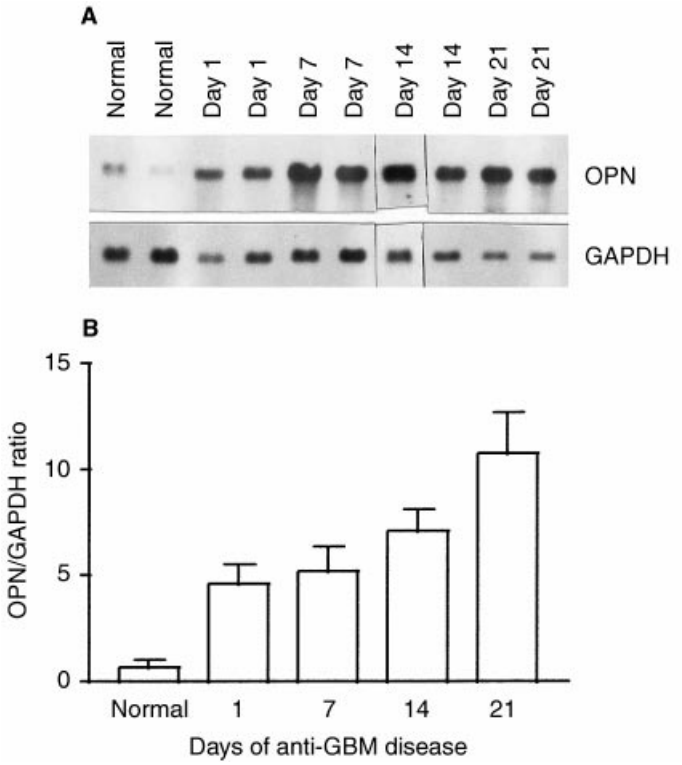

Fig. 1. Northern blot analysis of osteopontin (OPN) mRNA in normal and diseased rat kidney. (*A*) Detection of a single 1.6 kb OPN mRNA species in normal kidney and on days 1 to 21 of anti-GBM disease. Blots were reprobed for GAPDH. (*B*) Graph of the normalized OPN to GAPDH mRNA ratio.

aqueous medium. No signal was seen with the sense riboprobe labeled to the same specific activity.

Quantitation of *in situ* hybridization and immunohistochemistry staining

Positively stained cells were quantitated in tissue sections as previously described [32, 33]. Briefly, the number of cells labeled with the OPN cRNA probe or the different mAb were counted in at least 50 glomeruli cross-sections per animal. Interstitial ED1+ macrophages and R73+ T-cells were counted in at least 20 consecutive high power fields moving from outer cortex to inner cortex by means of a 0.02 mm^2 graticule fitted in the eyepiece of microscope. The number of tubules positive for OPN, CD44 or both molecules (CD44+OPN+) were scored from at least 1000 cortical tubules. In addition, a point counting technique was used to quantitate the number of interstitial ED1+ or R73+ cells surrounding OPN+ and OPN-tubules. Finally, OPN+ and OPN- cortical tubules were assessed for tubulitis by scoring the presence of OX-1+ leukocytes between and/or within the tubules in at least 1000 cortical tubules per animal. Data are expressed as the mean ± SEM for groups of six animals.

Statistical analyses

One way analysis of variance (ANOVA) from the Complete Statistical Analysis program (CSS, Statsoft, USA) was used to analyze differences in clinical data and quantitative immunohistochemistry scoring. The Pearson single correlation coefficient was used to compare OPN protein expression with macrophage and T cell accumulation, proteinuria and renal impairment. The relationship between OPN expression and glomerular and tubulointerstitial damage was compared using the Spearman's rank correlation coefficient.

Table 1. Histopathology in rat anti-GBM glomerulonephritis

Day of Disease	Glomerular hypercellularity (0–3)	Glom. segmental lesions %	Glomerular crescents %	Tubulointerstitial lesions %
Day 1	0.7 ± 0.1	12 ± 3.2	0	4.3 ± 0.5
Day 7	2.1 ± 0.2	25 ± 4.5	13.5 ± 1.1	12.5 ± 2.2
Day 14	2.5 ± 0.2	33 ± 3.5	32.6 ± 4.5	22.6 ± 2.8
Day 21	2.8 ± 0.3	46 ± 3.8	48.8 ± 5.1	38.5 ± 3.6

Data were obtained from groups of 6 animals (mean ± SEM).

RESULTS

Osteopontin expression in normal rat kidney

Northern blotting demonstrated constitutive expression of a single 1.6 kb species of OPN mRNA in normal rat kidney (Fig. 1A). *In situ* hybridization and antibody staining identified weak OPN mRNA and protein expression by occasional glomerular parietal epithelial cells and rare cells within the glomerular tuft (Figs. 2A, 3A, and 4A). In the tubulointerstitium, OPN mRNA and protein expression was largely restricted to the thick ascending limbs of the loop of Henle, accounting for less then 5% (3.3 ± 1.8%) of all cortical tubules (Figs. 2A, 3A, and 5A), whereas most medullary tubules exhibited weak OPN mRNA and protein expression. No staining was seen using the OPN sense control probe (not shown).

Up-regulation of osteopontin gene expression in anti-GBM disease

Northern blot analysis of whole kidney RNA demonstrated a 4.6-fold increase in OPN mRNA levels relative to GAPDH mRNA on day 1 of anti-GBM disease, and OPN mRNA levels continued to increase over the disease course (Fig. 1).

De novo glomerular OPN expression, leukocyte accumulation and crescent formation

Severe glomerular lesions developed over the 21 day course of rat anti-GBM glomerulonephritis, including: hypercellularity, segmental lesions and crescent formation (Table 1). *In situ* hybridization and immunostaining showed a significant increase in the number of OPN+ glomerular cells during the progression of the disease (Fig. 4A). Glomerular OPN expression was evident within focal and global lesions, with OPN+ cells identified as predominantly visceral epithelial cells, although a small number of ED1+ macrophages also showed OPN expression (Figs. 2B and 3B). An important observation was the *de novo* OPN expression by parietal epithelial cells on day 1 of disease, which became more prominent as the disease progressed over days 7 to 21. This *de novo* OPN expression was demonstrated by both *in situ* hybridization and immunohistochemistry (Figs. 2 B-E and 3C), and preceded the accumulation of ED1+ macrophages within Bowman's space beginning on day 7 of the disease. Examination of individual glomeruli found a clear association between increased OPN expression by parietal epithelial cells and ED1+ macrophage

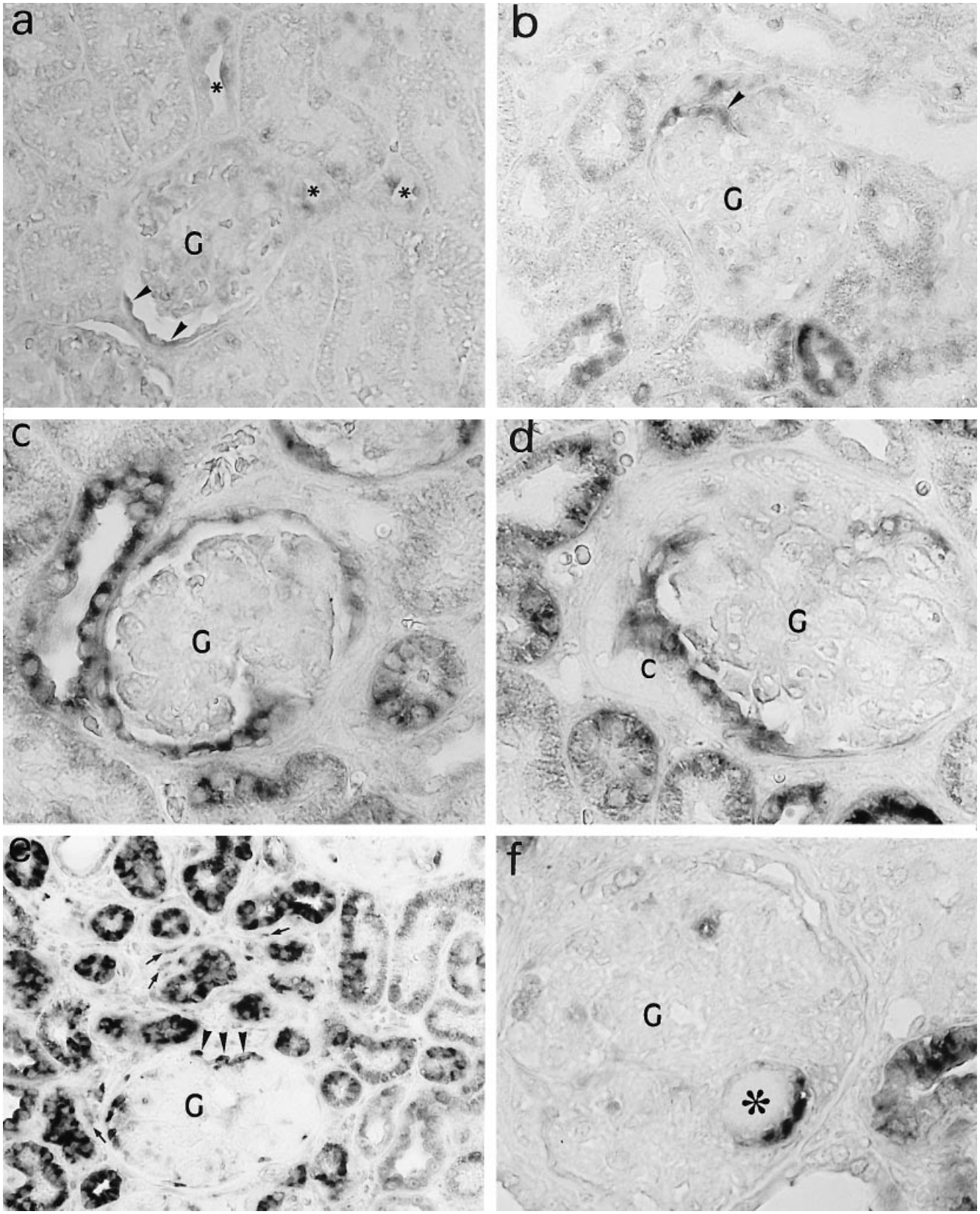

Fig. 2. Detection of osteopontin (OPN) mRNA by *in situ* hybridization in rat anti-GBM glomerulonephritis. (*A*) Normal rat kidney showing weak OPN mRNA expression by glomerular parietal epithelial cells (arrowheads) and thick ascending limbs of Henle (asterisks). (*B*) Increased OPN mRNA expression by glomerular parietal epithelial cells, podocytes (arrowhead) and some proximal tubules on day 1 of disease. (*C*) Day 7 showing strong up-regulation of OPN mRNA expression by glomerular parietal epithelial cells and proximal and distal tubules. (*D*) Day 14 showing marked OPN mRNA expression in a glomerular crescent (c). (*E*) Day 21 showing strong OPN mRNA expression by glomerular visceral epithelial cells (arrowheads) and atrophic tubules and spindle-shaped fibroblast-like cells (arrows) in an area of tubulointerstitial damage. (*F*) Day 21 showing OPN mRNA expression by a multinucleated giant cell (*) within a glomerular lesion. G, glomerulus. Original magnification ×250 (A-E) and ×400 (F).

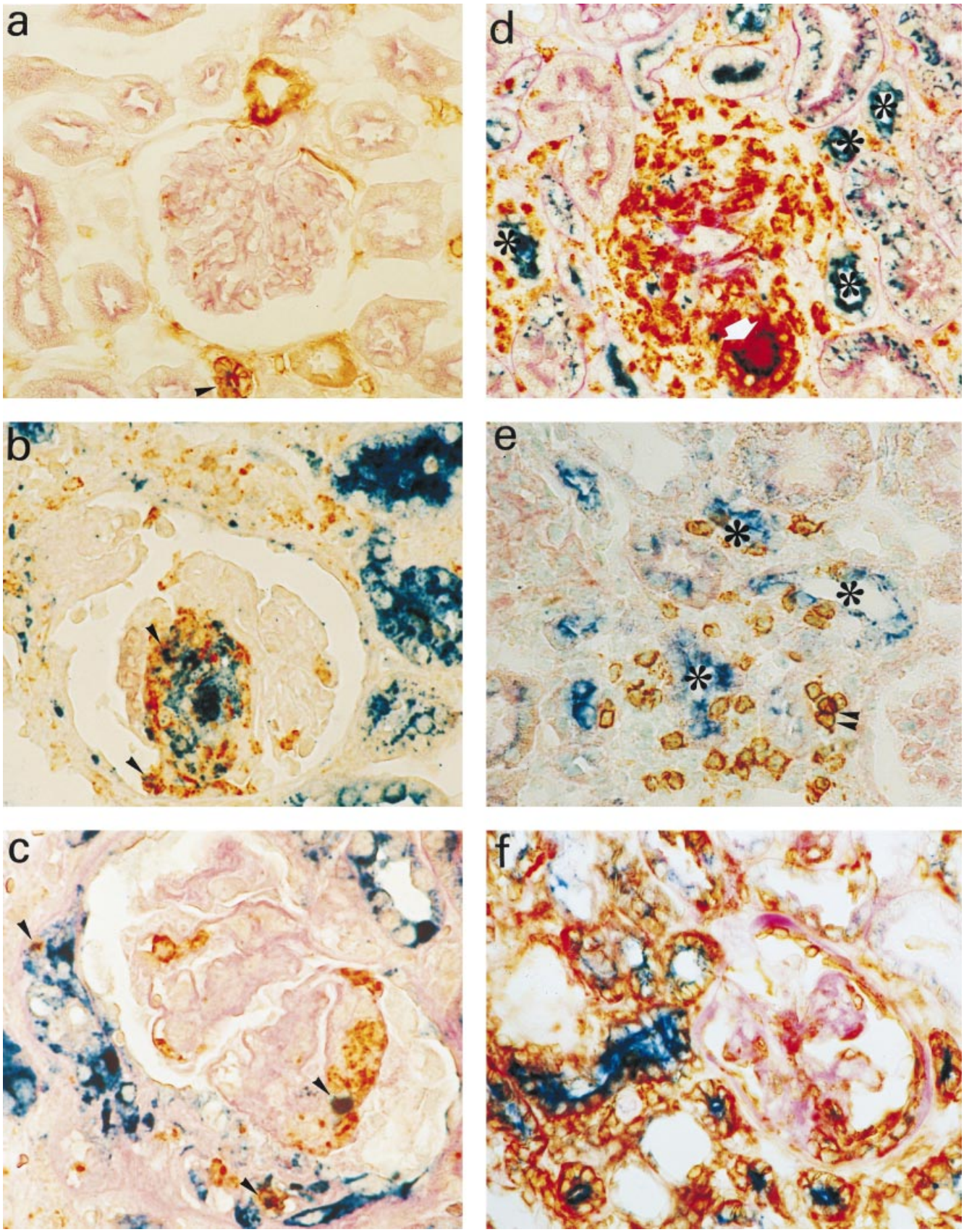
a
d
b
e
c
f

Fig. 3. Double immunohistochemistry staining of osteopontin (OPN) protein in normal kidney and rat crescentic glomerulonephritis. (*A*) Normal rat kidney showing co-localization of OPN (blue) and CD44 (brown) protein in thick ascending limbs of the loop of Henle (arrowhead). Some distal tubules show only CD44 expression. (*B*) Focal up-regulation of glomerular OPN protein expression (blue) and ED1+ macrophage accumulation (brown) in a focal segmental glomerular lesion. Note that some ED1+ macrophages are also OPN-positive. (*C*) Up-regulation of OPN expression by glomerular parietal epithelial cells (blue) and ED1+ macrophage accumulation (brown) in glomerular crescent formation. Some ED1+ macrophages are also OPN-positive. (*D*) Strong OPN expression by an ED1+ macrophage multinucleated giant cell (white arrow) within a granulomatous lesion on day 21 of disease. Note also strong OPN expression by tubules and in areas of tubulitis (*). (*E*) R73+ T-cells (brown) were localized within an area of tubulitis (*) exhibiting strong tubular OPN expression (blue). (*F*) Co-localization of OPN (blue) and CD44 (brown) within a glomerular crescent and an area of tubulointerstitial damage. Sections were counterstained with PAS minus hematoxylin. Original magnification ×400.

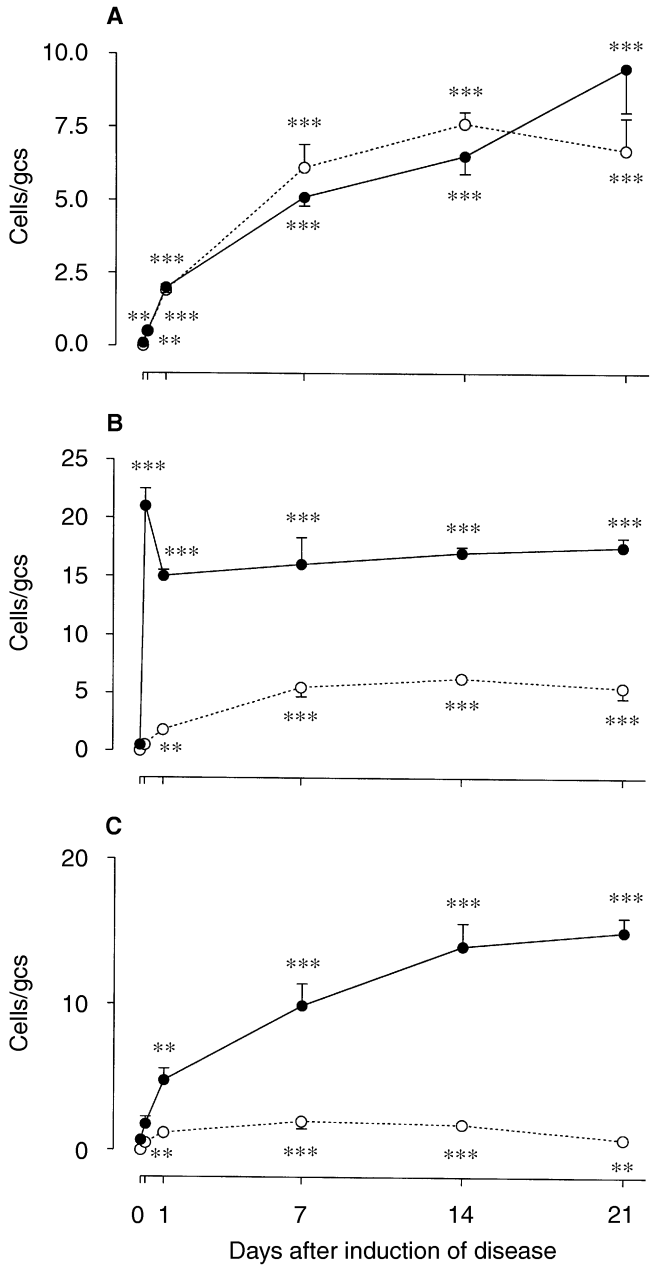

Fig. 4. Quantitation of glomerular osteopontin (OPN) and CD44 expression and leukocyte infiltration in rat anti-GBM glomerulonephritis. (*A*) Cells positive for OPN mRNA (●) or OPN protein (○); (*B*) glomerular CD44+ cells (●) and OPN+CD44+ double-positive cells (○); (*C*) glomerular ED1+ macrophages (●) and $R73^+$ T-cells (○). Data are expressed as the mean ± SEM from groups of 6 animals per glomerular cross-section (gcs). $^*P < 0.05$, $^{**}P < 0.01$, $^{***}P < 0.001$ compared to normal animals (day 0).

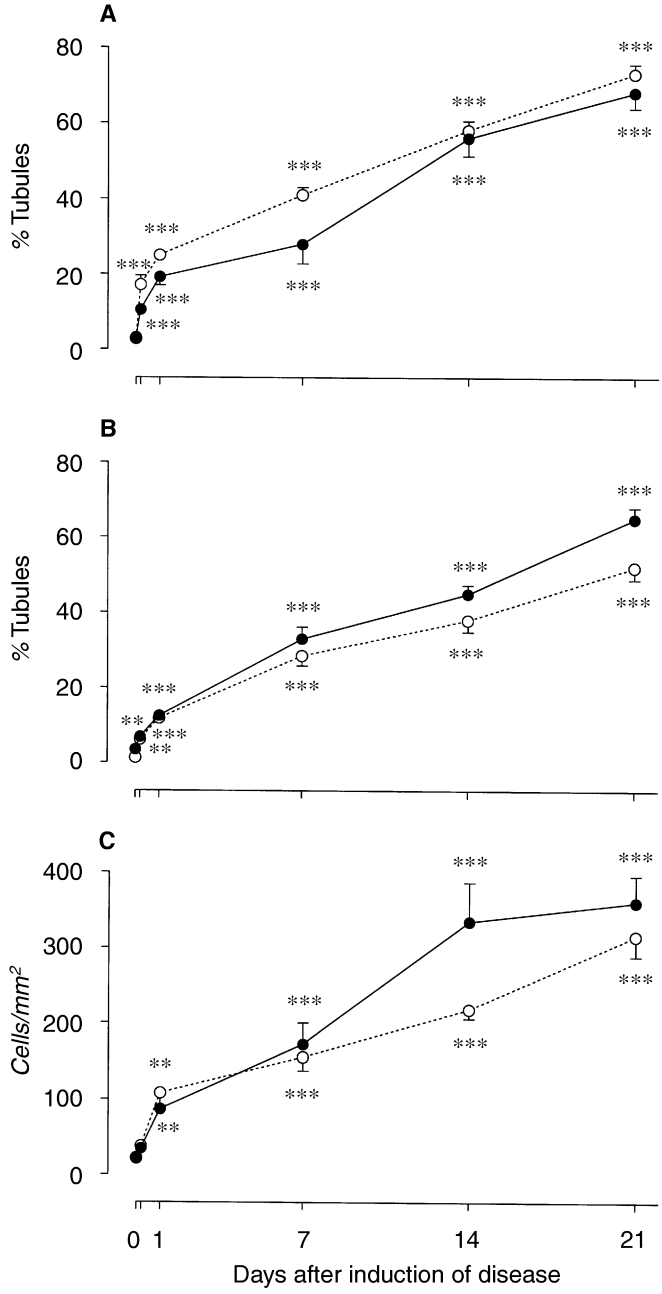

Fig. 5. Quantitation of tubular osteopontin (OPN) and CD44 expression and interstitial macrophage and T-cell accumulation in rat anti-GBM glomerulonephritis. (*A*) Tubules positive for OPN mRNA (●) and OPN protein (○); (*B*) CD44+ tubules (●) and OPN+CD44+ double-positive tubules (○); (*C*) interstitial ED1+ macrophages (●) and R73+ T-cells (○). Data are expressed as the mean ± SEM from groups of 6 animals. $^{**}P < 0.01$, $^{***}P < 0.001$ compared to normal animals (day 0).

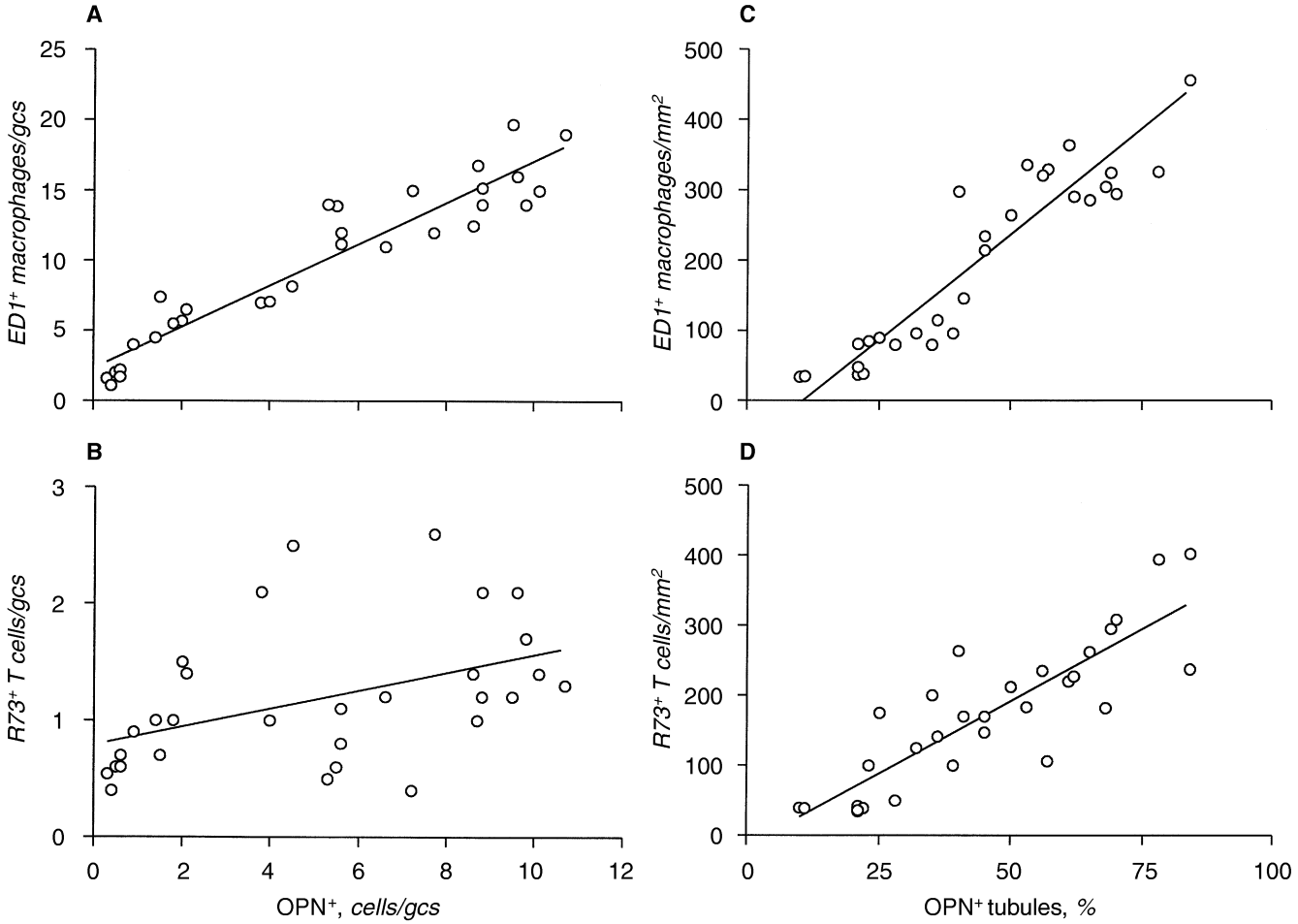

Fig. 6. Correlation analysis of leukocyte accumulation and osteopontin (OPN) expression over the 21 day time course of rat anti-GBM glomerulonephritis. (*A*) Glomerular ED1+ macrophages and OPN+ cells ($r = 0.946$; $P < 0.001$); (*B*) glomerular R73+ T-cells and OPN+ cells ($r = 0.451$; $P < 0.05$); (*C*) interstitial ED1+ macrophages and the percentage of OPN+ tubules ($r = 0.933$; $P < 0.001$); (*D*) interstitial R73+ T-cells and the percentage of OPN+ tubules ($r = 0.857$; $P < 0.001$). The Pearson correlation coefficient is shown.

accumulation within Bowman's space, contributing to crescent formation (Fig. 3C). In addition, some spindle-shaped fibroblast-like cells in fibrocellular crescents showed OPN expression. Quantitation of glomerular OPN+ cells, macrophages and T-cells over the entire disease course found a highly significant correlation between glomerular OPN expression and macrophage accumulation, and also a significant correlation between glomerular OPN expression and T-cell accumulation (Fig. 6 A, B).

An interesting observation was the strong OPN mRNA and protein expression seen in ED1+ macrophage multinucleated giant cells (MGC), which were present within granulomatous-like lesions (Figs. 2F and 3D). Osteopontin+ MGC were seen in both glomerular and interstitial lesions.

Up-regulation of tubular osteopontin expression, leukocyte accumulation and tubulointerstitial injury

Up-regulation of tubular OPN mRNA and protein expression was evident as early as three hours following administration of anti-GBM serum, and this continued to increase over the disease course (Fig. 5A). The up-regulation of tubular OPN expression preceded the development of significant macrophage infiltration on day 1, and paralleled macrophage accumulation over the rest of the disease course (Fig. 5). This early *de novo* OPN expression was seen in proximal tubules adjacent to the glomerular hilar area (Fig. 2B) and in tubules adjacent to glomeruli and arterioles. By day 7 there was a patchy, focal pattern of tubular OPN expression, with OPN expression seen in 55 to 85% of cortical tubules over days 14 to 21 (Fig. 5A).

In situ hybridization and double immunohistochemistry staining showed that the marked up-regulation of tubular OPN mRNA and protein expression occurred in areas of focal tubulointerstitial macrophage and T cell infiltration, tubulitis, tubular atrophy and tubulointerstitial fibrosis (Figs. 2E and 3E). There was a highly significant correlation between the number of OPN+ tubules and macrophage and T-cell accumulation within the cortical interstitial compartment (Fig. 6 C, D). Furthermore, quantitative analysis demonstrated that most infiltrating peritubular macrophages and T cells accumulated around OPN+ tubules (Fig. 7 A, B), and that the incidence of tubulitis was much greater in OPN+ tubules as compared to OPN-tubules (Fig. 7C). In contrast, there was little change in the constitutive OPN mRNA and protein expression in medullary tubules over the 21 day disease course.

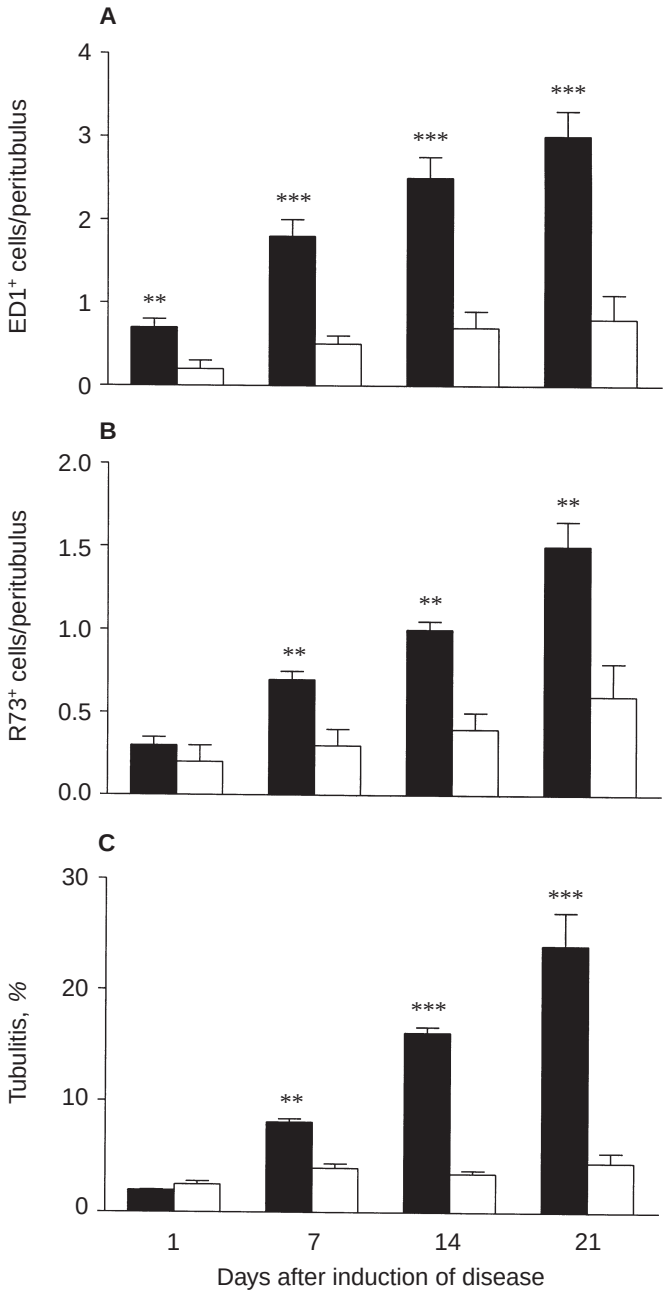

Fig. 7. Quantitation of tubular osteopontin (OPN) expression, interstitial macrophage and T-cell accumulation, and tubulitis in rat anti-GBM glomerulonephritis. (*A*) Peritubular accumulation of ED1+ macrophages around OPN+ tubules (■) and OPN-tubules (□). (*B*) Peritubular accumulation of R73+ T-cells around OPN+ tubules (■) and OPN-tubules (□). (*C*) The percentage of OPN+ tubules (■) and OPN-tubules (□) exhibiting tubulitis. Data are expressed as the mean ± SEM from groups of 6 animals. $^{*}P < 0.05$, $^{**}P < 0.001$.

Correlation of osteopontin expression with progressive renal injury

The number of OPN+ glomerular cells, parietal epithelial cells and cortical tubules was compared with histopathology and clinical disease parameters over the 21 day time course of anti-GBM glomerulonephritis. As shown in Table 2, the number of OPN+ cells in the glomerular tuft gave a significant correlation with glomerular hypercellularity, segmental lesions, proteinuria and loss of renal function. The number of OPN+ parietal epithelial cells correlated significantly with glomerular crescent formation, while the number of OPN+ cortical tubules correlated significantly with tubulointerstitial lesions, proteinuria and the loss of renal function.

Co-localization of osteopontin and CD44 expression

The relationship between expression of OPN and one of its ligands, CD44, was examined by double immunohistochemistry. Consistent with a previous study [33], immunostaining with the OX-50 mAb identified constitutive CD44 expression by parietal epithelial cells, occasional glomerular cells, medullary tubules and some thick ascending limbs of Henle in normal rat kidney. Most cortical and medullary CD44+ tubules also expressed OPN (Fig. 3A).

In anti-GBM disease, there was a rapid increase in the number of glomerular CD44+ cells at three hours after injection of anti-GBM serum (Fig. 4A). This was due to CD44 expression by the early, transient glomerular neutrophil infiltrate (not shown). From day 1 onwards, glomerular CD44 expression was due to infiltrating macrophages and resident glomerular visceral and parietal epithelial cells. In crescent formation, parietal epithelial cells expressed both CD44 and OPN, while macrophages within Bowman's space were mostly of a CD44+OPN-phenotype, as shown in Figure 3F.

There was also a marked increase in CD44 expression by cortical tubules in areas of tissue damage that paralleled the increase seen in tubular OPN expression, except during the first 24 hours in there was a more rapid up-regulation of tubular OPN expression compared to that of CD44 (Fig. 5B). Double staining showed that most OPN+ tubules also expressed CD44 (Fig. 3F). Interestingly, CD44 was expressed more strongly on the basolateral surface and tight junctions than on the luminal surface, whereas OPN was more prominent on the luminal surface and within the cytoplasm compared to the basolateral surface. CD44 was also expressed by most infiltrating interstitial leukocytes and by some spindle-shaped fibroblast-like cells.

DISCUSSION

In accord with previous studies, we have demonstrated constitutive OPN mRNA and protein expression in normal rat kidney [4, 18]. Although the function of OPN in normal kidney is not known, it has been proposed that OPN plays a role in preventing stone formation based upon the ability of OPN to inhibit calcium oxalate crystal formation *in vitro* [12].

A close association between the up-regulation of cortical tubular OPN expression and interstitial macrophage infiltration has been observed in a number of models of glomerular and interstitial nephritis [17–22]. Such an association was also demonstrated in the current study of rat anti-GBM glomerulonephritis, in which up-regulation of cortical tubular OPN expression preceded interstitial macrophage infiltration. Indeed, not only was there a highly significant correlation between up-regulation of tubular OPN expression and interstitial macrophage infiltration, but a significant correlation between interstitial T-cell infiltration and tubular OPN expression was also seen.

In renal disease models, most attention has focused upon the up-regulation of OPN expression by cortical tubules, but little is

Table 2. Correlation of OPN expression with histopathology and renal function in rat anti-GBM glomerulonephritis

OPN expression	Glom. Hypercell	Glom. seg. lesions	Glomerular crescents	Tubulointer. lesions	Proteinuria	Creatinine clearance
Glomerular tufts	0.85[b]	0.651[b]	—	—	0.687[b]	−0.728[b]
Parietal epithelial cells	—	—	0.743[b]	—	—	—
Tubules	—	—	—	0.759[b]	0.716[b]	0.571[a]

Abbreviations are: Glom, glomerular; Hypercell, hypercellularity, Seg, segmental; Tubulointer, tubulointerstitial.
Data from 30 animals were analyzed using the Pearson single correlation coefficient.
[a] $P < 0.01$, [b] $P < 0.001$

known of the potential role of OPN in the development of glomerular lesions. Weak OPN expression is evident by some parietal epithelial cells in normal kidney and an increase in OPN expression by the epithelial cells of Bowman's capsule has been noted in unilateral ureter obstruction and in glomerular undergoing sclerosis in aging mice [4, 20]. In addition, glomerular OPN mRNA expression has been reported in rat mesangioproliferative anti-Thy-1 nephritis at the time of glomerular macrophage accumulation, although this association was not examined in detail [18]. The current study has demonstrated marked up-regulation of OPN expression in severe glomerular lesions, suggesting that OPN contributes to the development of macrophage-induced segmental lesions, including crescent formation. Areas of focal glomerular macrophage accumulation were associated with focal OPN expression by predominantly visceral epithelial cells. It was notable that up-regulation of OPN expression by parietal epithelial cells occurred prior to macrophage accumulation within Bowman's space. Therefore, parietal epithelial cells may promote macrophage accumulation within Bowman's space either through the chemotactic activity of secreted OPN or the potent macrophage-adhesive property of cell-surface OPN [6, 13]. In addition, OPN expression by fibroblast-like cells suggest a role for OPN in the progression of crescents from a cellular to a fibrocellular phenotype.

One interesting observation was the strong OPN expression by macrophage MGC, while most infiltrating mononuclear macrophages had no detectable OPN expression. Given the potent adhesive properties of OPN for macrophages [6, 13], the expression of OPN on the surface of macrophages may promote cell-cell fusion during the formation of MGC. Indeed, examination of osteoclast formation supports this postulate. A study of osteophytic bone and inflammatory connective tissues found that mononuclear macrophages gained OPN mRNA expression when they changed from a non-specific esterase-positive phenotype to a tartrate-resistant acid phosphatase-positive phenotype during the formation of osteoclast MGC [34]. In addition, retinoic acid, which induces osteoclast formation, also up-regulates OPN mRNA in bone marrow-derived osteoclast precursors [35].

One ligand for OPN is CD44, a molecule which is expressed by infiltrating macrophages and T-cells and markedly up-regulated by intrinsic renal cells in the development of rat crescentic glomerulonephritis [33]. In the current study, examination of the relationship between OPN and CD44 expression provided two interesting results. First, a CD44-OPN interaction may promote leukocyte adhesion in the development of both tubulointerstitial and glomerular lesions, based upon the co-localization of CD44+ macrophages and T-cells with OPN+ tubular and glomerular epithelial cells. In addition, fibroblast migration into Bowman's space during the development of fibrocellular crescents may involve a CD44-OPN interaction. Second, an unexpected finding was that almost all glomerular and interstitial epithelial cells that expressed OPN also expressed CD44. This was evident in medullary tubules and collecting ducts in normal kidney, and in cortical tubules and glomerular parietal and visceral epithelial cells in areas of tissue damage in crescentic glomerulonephritis. These molecules may have distinct functional roles in the tubular response to injury, with OPN promoting recruitment and adhesion of macrophages and T-cells, whereas CD44 may promote epithelial cell adhesion to hyaluronan within the tubular basement membrane and facilitate epithelial cell-cell adhesion at tight junctions through a CD44-CD44 interaction mediated by a hyaluronan bridge, similar to that previously described for fibroblasts and mesangial cells [36, 37].

In summary, this study has identified a potential pathogenic role for OPN in macrophage and T-cell infiltration in the development of renal lesions in rat anti-GBM glomerulonephritis, including the formation of glomerular crescents and multinucleated giant cells. *In vivo* blocking studies are now required to provide functional evidence of the importance of OPN in the development of glomerular and tubulointerstitial damage in renal injury.

ACKNOWLEDGMENTS

This study was partly supported by grants from the Australian Kidney Foundation (G18/97), the National Health and Medical Research Council of Australia (940509), Guangdon Science and Technology Council of China (95015), and US Public Health Services (DK-47659 and DK-43422). This data were presented in part at the Annual Meeting of the American Society of Nephrology, New, Orleans, 1996.

Reprint requests to Dr. Hui Y. Lan, Department of Nephrology, Monash Medical Centre, 246 Clayton Road, Clayton, Victoria 3168, Australia.

APPENDIX

Abbreviations used in this article are: OPN, osteopontin; GBM, glomerular basement membrane; CD44, ligand to osteopontin; RGD, arginine-glycine-aspartic acid; PAS, Periodic acid-Schiff reagent; mAb, monoclonal antibodies; PAP, peroxidase anti-peroxidase complexes; APAAP, alkaline phosphatase anti-allkaline phosphatase complexes; DIG, digoxigenin; GAPDH, glyceraldehyde-3-phosphate dehydrogenase; MCG, multinucleated giant cells.

REFERENCES

1. Butler WT: Structural and functional domains of osteopontin. *Ann NY Acad Sci USA* 760:6–11, 1993
2. Denhardt DT, Guo X: Osteopontin: A protein with diverse functions. *FASEB J* 7:1475–1482, 1993
3. Brown LF, Berse B, Van De Water L, Papadopoulos-Sergiou A, Perruzzi CA, Manseau EJ, Dvorak HF, Senger DR: Expression and distribution of osteopontin in human tissues: Widespread association with luminal epithelial surfaces. *Mol Biol Cell* 3:1169–1180, 1992
4. Lopez CA, Hoyer JR, Wilson PD, Waterhouse P, Denhardt DT: Heterogeneity of osteopontin expression among nephrons in mouse

kidneys and enhanced expression in sclerotic glomeruli. *Lab Invest* 69:355–363, 1993
5. Miyazaki Y, Setoguchi M, Yoshida S, Higuchi Y, Akizuki S, Yamamoto S: The mouse osteopontin gene. Expression in monocytic lineages and complete nucleotide sequence. *J Biol Chem* 265:14432–14438, 1990
6. Patarca R, Freeman GJ, Singh RP, Wei FY, Durfee T, Blattner F, Regnier DC, Kozak CA, Mock BA, Morse HC, 3D, Et AL: Structural and functional studies of the early T lymphocyte activation 1 (Eta-1) gene. Definition of a novel T cell-dependent response associated with genetic resistance to bacterial infection. *J Exp Med* 170:145–161, 1989
7. Giachelli C, Bae N, Lombardi D, Majesky M, Schwartz S: Molecular cloning and characterization of 2B7, a rat mRNA which distinguishes smooth muscle cell phenotypes in vitro and is identical to osteopontin (secreted phosphoprotein I, 2aR). *Biochem Biophys Res Commun* 177:867–873, 1991
8. Senger DR, Perruzzi CA, Gracey CF, Papadopoulos A, Tenen DG: Secreted phosphoproteins associated with neoplastic transformation: Close homology with plasma proteins cleaved during blood coagulation. *Cancer Res* 48:5770–5774, 1988
9. Weber GF, Ashkar S, Glimcher MJ, Cantor H: Receptor-ligand interaction between CD44 and osteopontin (Eta-1). *Science* 271:509–512, 1996
10. Reinholt FP, Hultenby K, Oldberg A, Heinegard D: Osteopontin–A possible anchor of osteoclasts to bone. *Proc Natl Acad Sci USA* 87:4473–4475, 1990
11. Ross FP, Chappel J, Alvarez JI, Sander D, Butler WT, Farach-Carson MC, Mintz KA, Robey PG, Teitelbaum SL, Cheresh DA: Interactions between the bone matrix proteins osteopontin and bone sialoprotein and the osteoclast integrin alpha v beta 3 potentiate bone resorption. *J Biol Chem* 268:9901–9907, 1993
12. Shiraga H, Min W, Vandusen WJ, Clayman MD, Miner D, Terrell CH, Sherbotie JR, Foreman JW, Przysiecki C, Neilson EG, Hoyer JR: Inhibition of calcium oxalate crystal growth in vitro by uropontin: Another member of the aspartic acid-rich protein superfamily. *Proc Natl Acad Sci USA* 89:426–430, 1992
13. Singh RP, Patarca R, Schwartz J, Singh P, Cantor H: Definition of a specific interaction between the early T lymphocyte activation 1 (Eta-1) protein and murine macrophages in vitro and its effect upon macrophages in vivo. *J Exp Med* 171:1931–1942, 1990
14. Liaw L, Almeida M, Hart CE, Schwartz SM, Giachelli CM: Osteopontin promotes vascular cell adhesion and spreading and is chemotactic for smooth muscle cells in vitro. *Circ Res* 74:214–224, 1994
15. Senger DR, Perruzzi CA: Cell migration promoted by a potent GRGDS-containing thrombin-cleavage fragment of osteopontin. *Biochem Biophys Acta* 1314:13–24, 1996
16. Nikolic-Paterson DJ, Lan HY, Atkins RC: Macrophages in immune renal injury, in *Immunologic Renal Diseases*, edited by Neilson EG, Couser WG, Philadelphia, Lippincott-Raven, 1997, p 575
17. Giachelli CM, Pichler R, Lombardi D, Denhardt DT, Alpers CE, Schwartz SM, Johnson RJ: Osteopontin expression in angiotensin II-induced tubulointerstitial nephritis. *Kidney Int* 45:515–524, 1994
18. Pichler R, Giachelli CM, Lombardi D, Pippin J, Gordon K, Alpers CE, Schwartz SM, Johnson RJ: Tubulointerstitial disease in glomerulonephritis. Potential role of osteopontin (uropontin). *Am J Pathol* 144:915–926, 1994
19. Pichler RH, Franceschini N, Young BA, Hugo C, Andoh TF, Burdmann EA, Shankland SJ, Alpers CE, Bennett WM, Couser WG, Johnson RJ: Pathogenesis of cyclosporine nephropathy: Roles of angiotensin II and osteopontin. *J Am Soc Nephrol* 6:1186–1196, 1995
20. Diamond JR, Kees-Folts D, Ricardo SD, Pruznak A, Eufemio M: Early and persistent up-regulated expression of renal cortical osteopontin in experimental hydronephrosis. *Am J Pathol* 146:1455–1466, 1995
21. Eddy AA, Giachelli CM: Renal expression of genes that promote interstitial inflammation and fibrosis in rats with protein-overload proteinuria. *Kidney Int* 47:1546–1557, 1995
22. Kleinman JG, Worcester EM, Beshensky AM, Sheridan AM, Bonventre JV, Brown D: Upregulation of osteopontin expression by ischemia in rat kidney. *Ann NY Acad Sci* 760:321–323, 1995
23. Lan HY, Paterson DJ, Atkins RC: Initiation and evolution of interstitial leukocytic infiltration in experimental glomerulonephritis. *Kidney Int* 40:425–433, 1991
24. Dijkstra CD, Dopp EA, Joling P, Kraal G: The heterogeneity of mononuclear phagocytes in lymphoid organs: Distinct macrophage subpopulations in the rat recognized by monoclonal antibodies ED1, ED2 and ED3. *Immunology* 54:589–599, 1985
25. Damoiseaux JG, Dopp EA, Calame W, Chao D, MacPherson GG, Dijkstra CD: Rat macrophage lysosomal membrane antigen recognized by monoclonal antibody ED1. *Immunology* 83:140–147, 1994
26. Hunig T, Wallny HJ, Hartley JK, Lawetzky A, Tiefenthaler G: A monoclonal antibody to a constant determinant of the rat T cell antigen receptor that induces T cell activation. Differential reactivity with subsets of immature and mature T lymphocytes. *J Exp Med* 169:73–86, 1989
27. Paterson DJ, Jefferies WA, Green JR, Brandon MR, Corthesy P, Puklavec M, Williams AF: Antigens of activated rat T lymphocytes including a molecule of 50.000 Mr detected only on CD4 positive T blasts. *Mol Immunol* 24:1281–1290, 1987
28. Zheng Z, Katoh S, He Q, Oritani K, Miyake K, Lesley J, Hyman R, Hamik A, Parkhouse RM, Farr AG, Kincade PW: Monoclonal antibodies to CD44 and their influence on hyaluronan recognition. *J Cell Biol* 130:485–495, 1995
29. Lan HY, Mu W, Nikolic-Paterson DJ, Atkins RC: A novel, simple, reliable, and sensitive method for multiple immunoenzyme staining: Use of microwave oven heating to block antibody crossreactivity and retrieve antigens. *J Histochem Cytochem* 43:97–102, 1995
30. Hattori M, Nikolic-Paterson DJ, Lan HY, Kawaguchi H, Ito K, Atkins RC: Up-regulation of ICAM-1 and VCAM-1 expression during macrophage recruitment in lipid induced glomerular injury in ExHC rats. *Nephrology* 1:221–232, 1995
31. Lan HY, Mu W, Ng Y-Y, Nikolic-Paterson DJ, Atkins RC: A simple, reliable, and sensitive method of nonradioactive in situ hybridization: Use of microwave heating to improve hybridization efficiency and preserve tissue morphology. *J Histochem Cytochem* 44:281–287, 1996
32. Lan HY, Mu W, Yang N, Meinhardt A, Nikolic-Paterson DJ, Bacher M, Atkins RC, Bucala R: De novo renal expression of macrophage migration inhibitory factor (MIF) during the development of rat crescentic glomerulonephritis. *Am J Pathol* 149:1119–1127, 1996
33. Jun Z, Hill PA, Lan HY, Foti R, Mu W, Atkins RC, Nikolic-Paterson DJ: CD44 and hyaluronan expression in the development of experimental crescentic glomerulonephritis. *Clin Exp Immunol* 108:69–77, 1997
34. Connor JR, Dodds RA, James IE, Gowen M: Human osteoclast and giant cell differentiation: The apparent switch from nonspecific esterase to tartrate resistant acid phosphatase activity coincides with the in situ expression of osteopontin mRNA. *J Histochem Cytochem* 43: 1193–1201, 1995
35. Kaji H, Sugimoto T, Kanatani M, Fukase M, Kumegawa M, Chihara K: Retinoic acid induces osteoclast-like cell formation by directly acting on hemopoietic blast cells and stimulates osteopontin mRNA expression in isolated osteoclasts. *Life Sci* 56:1903–1913, 1995
36. Green SJ, Tarone G, Underhill CB: Aggregation of macrophages and fibroblasts in inhibited by a monoclonal antibody to the hyaluronate receptor. *Exp Cell Res* 178:224–232, 1988
37. Nikolic-Paterson DJ, Jun Z, Tesch GH, Lan HY, Foti R, Atkins RC: De novo CD44 expression by proliferating mesangial cells in rat anti-Thy-1 nephritis. *J Am Soc Nephrol* 7:1006–1014, 1996